Journal of
Marine Science and Engineering

MDPI

Article

Analysis of Downstream Sediment Transport Trends Based on In Situ Data and Numerical Simulation

Yuxi Wu [1,2], Xiwen Li [1,*], Enjin Zhao [2,3,4,*], Yang Wang [1], Shiyou Zhang [1], Zhiming Xu [5], Qinjun Wang [5], Dongxu Jiang [1] and Zhuang Xing [1]

1 Haikou Marine Geological Survey Center, China Geological Survey, Haikou 571127, China; yuxiwu@cug.edu.cn (Y.W.); wangyang01@mail.cgs.gov.cn (Y.W.); 17608918675@163.com (S.Z.); 13078929611@163.com (D.J.); 17683345561@163.com (Z.X.)
2 College of Marine Science and Technology, China University of Geosciences, Wuhan 430074, China
3 Shenzhen Research Institute, China University of Geosciences, Shenzhen 518057, China
4 Shandong Provincial Key Laboratory of Marine Environment and Geological Engineering, Ocean University of China, Qingdao 266100, China
5 Unit 91656 of the Chinese People's Liberation Army, Shanghai 200231, China; 18606629153@163.com (Z.X.); wyx959022104@icloud.com (Q.W.)
* Correspondence: author: lxw1818168@163.com (X.L.); zhaoej@cug.edu.cn (E.Z.)

Abstract: This study conducted an in-depth analysis of the sediment dynamics in the lower reaches of the Changhua River and its estuary on Hainan Island. Through field collection of topographic data and sediment sampling, combined with advanced computational techniques, the study explored the transport pathways and depositional patterns of sediments. The grain size trend analysis (GSTA) method was utilized, in conjunction with the Flemming triangle diagram method, to classify the dynamic environment of the sediments. Furthermore, hydrodynamic modeling results were integrated to further analyze the transport trends of the sediments. The study revealed that the sediment types in the research area are complex, primarily consisting of gravelly sand and sandy gravel, indicating a generally coarse sedimentary environment in the region. The sediments in the lower reaches of the Changhua River generally transport towards the south and southwest (in the direction of Beili Bay). The net sediment transport directions inferred from the GSTA model are largely consistent with the Eulerian residual flow patterns, especially in the offshore area, where discrepancies are observed in the nearshore zone. The nearshore transport is influenced by the combined effects of alongshore currents, residual flows, and river inputs, while the offshore transport exhibits a shift from the northwest to southwest directions, reflecting the regional circulation patterns.

Keywords: sediment grain size characteristics; sediment transport trends; Gao–Collins method; hydrodynamic; Changhua River estuary

Citation: Wu, Y.; Li, X.; Zhao, E.; Wang, Y.; Zhang, S.; Xu, Z.; Wang, Q.; Jiang, D.; Xing, Z. Analysis of Downstream Sediment Transport Trends Based on In Situ Data and Numerical Simulation. *J. Mar. Sci. Eng.* **2024**, *12*, 1982. https://doi.org/10.3390/jmse12111982

Academic Editor: Gemma Aiello

Received: 15 October 2024
Revised: 30 October 2024
Accepted: 1 November 2024
Published: 2 November 2024

1. Introduction

In recent years, with the advancement in marine scientific research [1–6], sediment grain size analysis techniques have been extensively applied [7–12]. Grain size parameters, such as mean grain size, sorting coefficient, and skewness, have been established as effective indicators for reflecting the provenance, transportation, and depositional environment of sediments [13–15]. Concurrently, the continuous refinement of sediment dynamic zoning and sediment transport trend analysis methods has provided robust tools for uncovering sedimentary processes [16,17]. The transport process of sediments not only reflects the complexity and variability of the regional hydrodynamic environment, but also significantly impacts regional geomorphological evolution, ecological environments, and resource development and utilization [18]. The grain size characteristics and distribution of sediments are key parameters for revealing sediment transport

patterns, and detailed grain size analysis can provide an in-depth understanding of the sources, transport pathways, and depositional mechanisms of sediments [19]. It is against this technological backdrop that we are able to more meticulously explore the transport patterns of sediments in specific areas, such as the lower reaches of the Changhua River, and their environmental impacts.

In the exploration of sediment transport directions in the lower reaches of the Changhua River, the issue of sediment accumulation, as one of the core challenges in the field of water conservancy projects, cannot be overlooked due to its complex causes and the urgency of its management [20]. The Gao–Collins method, a two-dimensional sediment grain size trend analysis model, has been widely applied in various marine environments to infer net sediment transport patterns from the spatial distribution of grain size parameters [21–23]. Yet, its application in the Changhua River estuary has been sparse, and the results have not been fully synthesized with the local hydrodynamic conditions and sediment sources [12,24]. With the rapid development of computational technology, sediment transport models, particularly the GSTA (grain size trend analysis) model, have provided a powerful tool for accurately simulating and predicting the dynamic processes of river sediments [25–27]. The GSTA model, an evolution of the Gao–Collins method, incorporates advanced computational techniques to enhance the accuracy and resolution of sediment transport predictions [28–30]. The GSTA model not only integrates classical hydrodynamics theory with modern numerical simulation techniques, but also innovatively considers the coupled effects of topographical changes, flow conditions, sediment grain size distribution, and riverbed morphology, providing a more comprehensive and accurate reflection of sediment transport and deposition processes within river systems.

The lower reaches of the Changhua River in Hainan Island and its estuary, a critical transition zone between terrestrial and marine systems, have been subject to complex hydrodynamic conditions shaped by fluvial inputs, tidal actions, and wave energies [12,24,31]. These conditions are further influenced by the presence of dams upstream, which regulate the river's flow and significantly impact sediment transport patterns. The water discharge data used in our hydrodynamic model, sourced from the nearest Baoqiao Hydrological Station, captures the regulatory role of these dams, ensuring that our analysis reflects the real-world conditions influenced by their presence. The lower reaches of the Changhua River, characterized by low-lying terrain, suffer from severe sediment accumulation, which not only restricts the river's flood discharge capacity, increasing the risk of flood disasters, but also directly threatens the safety of the lives and property of surrounding residents and agricultural production [32,33]. Additionally, the land use patterns within the basin significantly influence the sediment dynamics. According to recent research, the predominant land use types in the Changhua River basin include arable land, forest land, and urban areas, with significant changes observed over the past two decades [34,35]. Arable land, primarily distributed in coastal areas, and forest land, mainly in the central mountainous regions (Figure 1), have experienced fluctuations that reflect the interplay between natural conditions and human activities. These changes directly affect the generation and transport of sediment, exacerbating the sediment accumulation issues in the lower reaches. Therefore, in-depth research on the transport direction of sediments in the lower reaches of the Changhua River is crucial for understanding the spatiotemporal distribution characteristics of sediment accumulation, evaluating the effectiveness of river channel regulation projects, and formulating scientific management measures.

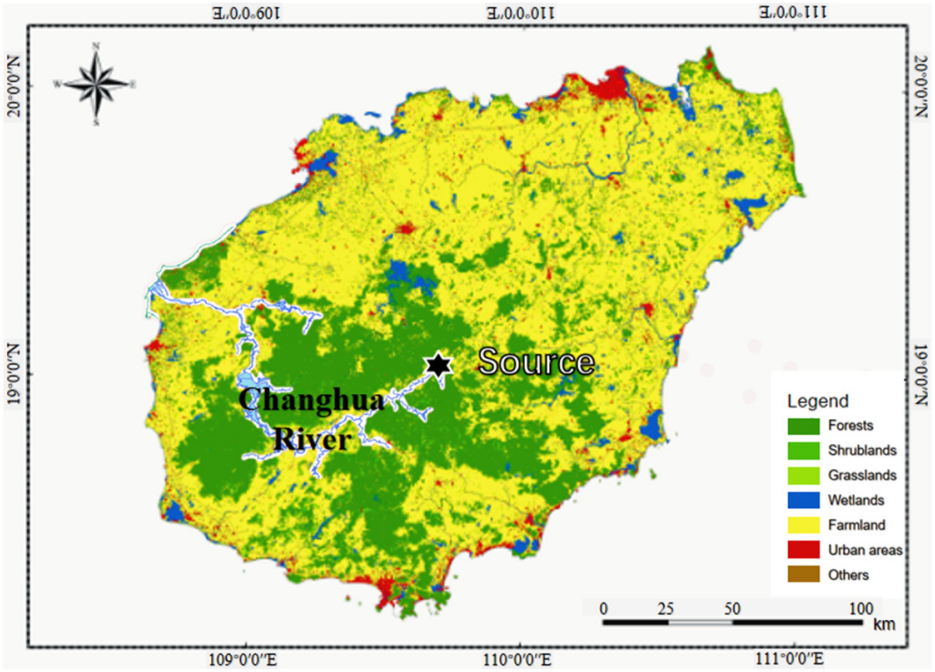

Figure 1. Land use patterns in Hainan province with a focus on the Changhua River Basin, the black star refers to the source of the Changhua River (Origin: International Research Center of Big Data for Sustainable Development Goals. DOI: 10.12237/casearth.63eb24d7819aec795e09af68. [36]).

The application of the GSTA model will enable us to more accurately simulate the sediment transport processes in the lower reaches of the Changhua River under different seasonal and flow conditions, revealing the transport patterns of sediments in the river channel and predicting potential future accumulation trends. This will provide a scientific basis and technical support for river channel regulation, flood control planning, navigation safety, and ecological environment protection in the lower reaches of the Changhua River. Additionally, through the simulation analysis of the GSTA model, we can evaluate the effectiveness of different management measures, optimize resource allocation, and achieve sustainable development in the lower reaches of the Changhua River. Furthermore, the incorporation of hydrodynamic modeling in this study allows for a detailed analysis of sediment transport trends by simulating the complex interactions between flow velocity and direction, which are crucial for understanding the net transport patterns in the lower reaches of the Changhua River.

Building on the achievements of previous research, this study, in conjunction with the actual conditions of the lower reaches of the Changhua River and the nearby sea area of the river mouth, employs the Flemming triangle diagram method and the GSTA model. Focusing on the surface sediments of the lower reaches of the Changhua River and the nearby sea area of the river mouth, the study aims to explore the transport direction and dcontrolling factors of sediments in the area through grain size analysis, sediment type classification, and dynamic environmental zoning. Additionally, it will utilize the residual current from hydrodynamic modeling to further analyze the transport of sediments, providing a more comprehensive understanding of the sediment dynamics in the study area.

2. Study Area and Data

The study area is situated in the western part of Hainan Island, mainly encompassing the lower reaches of the Changhua River and its estuary (Figure 2). The approximate coordinates range from 108°36′ E to 108°50′ E and 19°15′ N to 19°22′ N. The study area covers a large part of the region from Chahe Town to the estuary of the Changhua River, including Xiantiancun, Dangchangcun and Jiuxiancun, among others. A total

of 40 offshore sampling points were investigated and collected by the Haikou Geological Survey Center. Sediment data for the open sea were obtained through historical data [24,32,33,37].

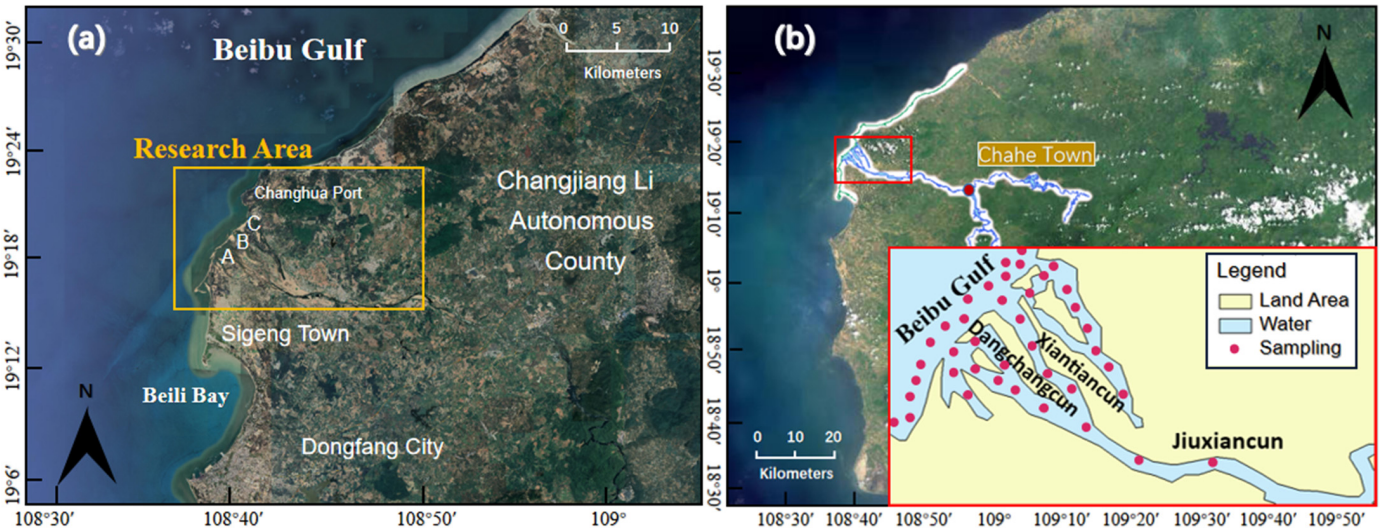

Figure 2. Geographical extent of the study area in the lower reaches of the Changhua River and its estuary, highlighting the key sampling locations and topographical features that influence sediment transport dynamics: (**a**) Orange Box Denotes the Study Area with 3 Major Estuaries (A, B, C), and Changhua Port Located at Estuary C. (**b**) Red Box Encompasses Villages and 40 Sampling Points Within the Study Area.

The hydrological regime of the lower Changhua River is characterized by a distinct seasonal variability, with a pronounced flood season typically occurring from May to October and a dry season from November to April [38]. The river's discharge is highly variable, with the flood season accounting for approximately 77% of the annual net flow [39–43]. The estuary, shaped by the river's dynamic interaction with tidal and wave forces, exhibits a weak tidal regime with a mean tidal range of less than 2 m, indicating the dominance of fluvial inputs over tidal influences [32,44]. The river's sediment is predominantly coarse-grained, reflecting its strong erosional capacity, particularly during the flood season when high discharges lead to significant sediment mobilization and transport [32,35]. Figure 3 illustrates the long-term dynamics of the relationship between water discharge and sediment transport in the lower reaches of the Changhua River. This figure presents the annual discharge, sediment concentration, and sediment transport rate, highlighting the seasonal variability and the dominant factors influencing sediment movement. The data reveal a pronounced flood season from May to October, during which approximately 77% of the annual net flow occurs, significantly impacting sediment mobilization and transport. The dry season, from November to April, shows a marked decrease in both water discharge and sediment transport, indicating the critical role of seasonal hydrological patterns in shaping sediment dynamics.

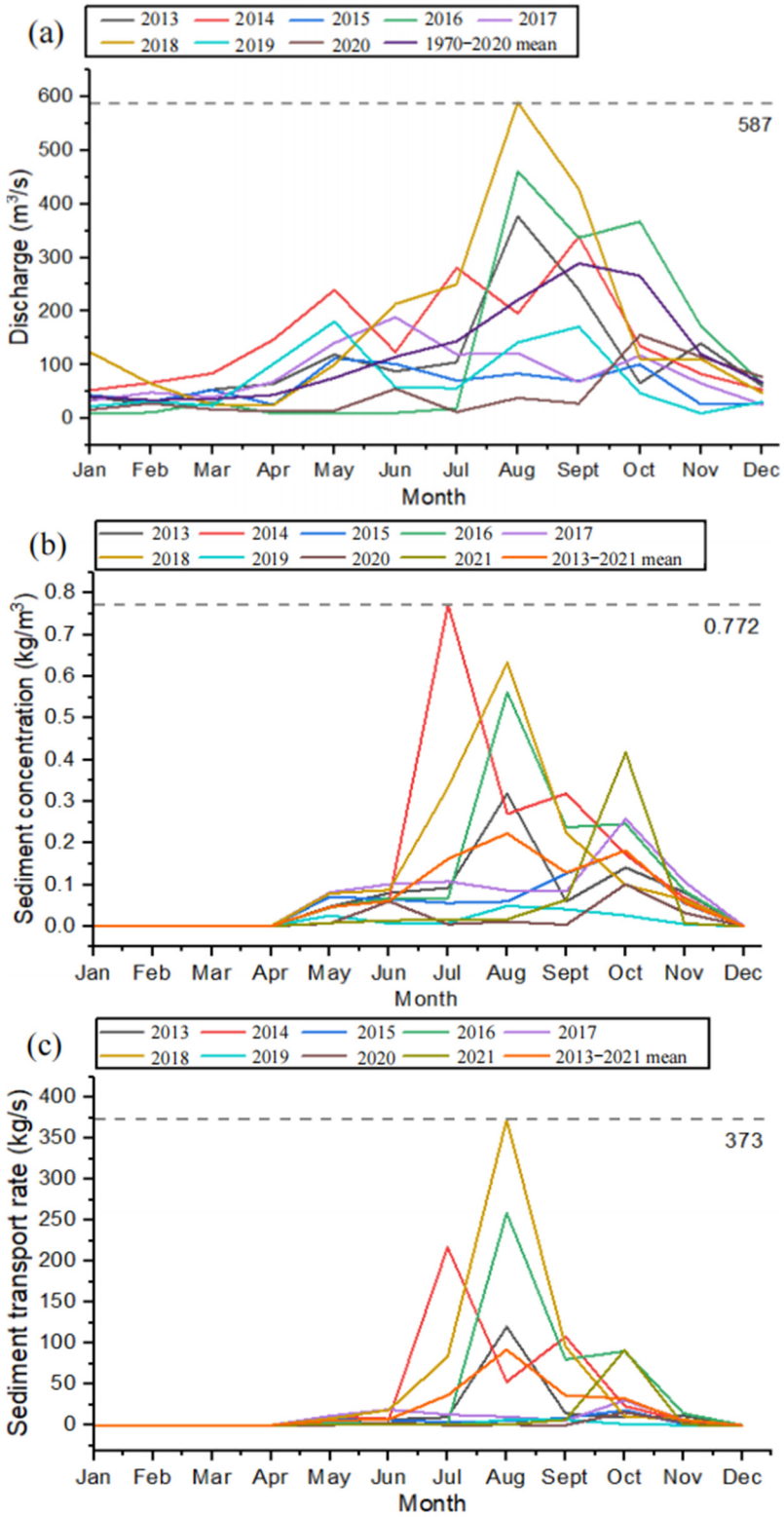

Figure 3. (**a**) Annual Discharge in the Lower Reaches of the Changhua River: The maximum value of 587 m^3/s occurred in August 2018. (**b**) Annual Sediment Concentration in the Lower Reaches of the Changhua River: The maximum value of 0.772 kg/m^3 was recorded in July 2014. (**c**) Annual Sediment Transport Rate in the Lower Reaches of the Changhua River: The maximum value of 373 kg/s was reached in August 2018.

3. Materials and Methods

3.1. Sediment Sampling

Sediment grain size analysis was conducted at the Hainan Provincial Research Center for Geological Testing. Initially, an appropriate amount of the original sample was thoroughly mixed and uniformly dried at 80 °C. For samples with particle sizes less than 2000 μm, a suitable amount of the sample was treated with 10 mL of hydrogen peroxide and hydrochloric acid solutions to remove organic matter and calcareous biomaterials, respectively. Subsequently, 0.05 N sodium hexametaphosphate was added, and the mixture was allowed to stand in a beaker for 24 h. Afterward, it was sonicated for 15 min using an ultrasonic oscillator and then analyzed using a Master-sizer 2000 laser particle size analyzer. The measurement range of this analyzer is 0.02 to 2000 μm, with a relative error of less than 2%, a particle size resolution of 0.01Φ, and a repeatability relative error of less than 3%. The data from both parts were merged using a laser diffraction particle size analyzer simulation program to obtain a complete particle size distribution.

To evaluate the sensitivity of the sample point selection, we conducted additional analyses. By varying the number of sample points, we found that the results remained robust within a certain range: we set up multiple groups with different quantities of sample points and observed the changes in the Flemming triangle diagram. When the number of sample points was reduced by 20%, the results exhibited minimal variation, consistent with those obtained using the full set of sample points in terms of the dynamical partitioning. This indicates that our sample point selection is representative to a certain extent and that the research findings possess high robustness. Figure 4 illustrates three scenarios: all sampling points, a 20% reduction in sampling points, and a 40% reduction in sampling points.

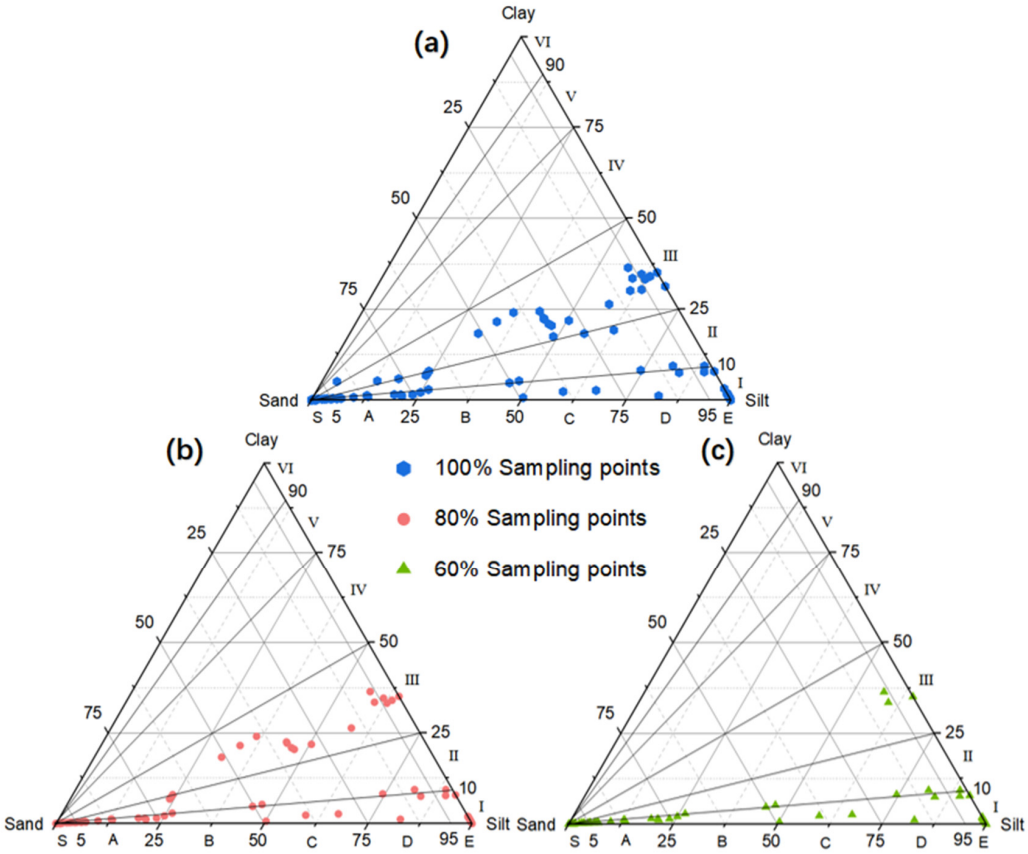

Figure 4. The Flemming Triangle Diagram under Different Numbers of Sample Points: (**a**) The blue hexagons represent the distribution of the original sampling points, serving as the control group. (**b**) The red dots indicate the distribution of 80% of the sampling points. (**c**) The green triangles show the distribution of 60% of the sampling points.

The sample particle sizes were expressed using the Udden–Wentworth scale in phi (Φ) units. The mean particle size (Mz), sorting coefficient (δ), and skewness (Sk) were calculated using the Folk–Ward graphical method with corresponding formulae [13].

3.2. GSTA Model for Sediment Transport Trend Analysis

The planar distribution trend of sediment grain size parameters is known as the grain size trend. By comparing the grain size parameters at a given point with those of its surrounding points, the possible direction of the net transport can be determined. In the case of any two adjacent sampling points, based on sediment grain size parameters such as the mean grain size, sorting coefficient and skewness, a grain size trend vector can be defined, which is a unit vector from the sampling point to the point of interest [29].

A characteristic distance is used to determine whether two sampling points are adjacent. The characteristic distance is usually defined by the maximum sampling interval (or geostatistical distance) and should first be determined to assess the nearest neighbors of a sampling site [22,23]. In this paper, the characteristic distance chosen is the maximum sampling interval. Based on the aforementioned grain size trend vector conditions, all grain size trend vectors between the sampling point and its adjacent sampling points can be obtained. Then, by summing all the grain size trend vectors at this point, the resultant vector for this sampling point can be derived. The length only indicates the significance of this particle size trend, not its magnitude. Its direction represents the net transport direction of sediments at the sampling point [28].

3.3. Hydrodynamic Modeling

In the study, bathymetric data are derived from ETOPO1 global seafloor topography data and in situ measurements using ADCP. The spatial resolution of ETOPO1 data is $1/60^\circ \times 1/60^\circ$, which is insufficient for the research requirements. ADCP depth measurements have higher density in nearshore areas and provide actual measured data with higher accuracy.

The model's open boundary conditions are defined by the forced tidal water level, incorporating eight primary tidal components: M2, S2, K1, O1, N2, K2, P1, and Q1. The open boundary water level is dynamically adjusted to match simulation outcomes. The model's closed boundary aligns with the terrestrial boundary, where the normal velocity of ocean currents is set to zero, precluding any exchange of temperature and salt between land and seawater. The model also integrates the impact of wind fields, with data sourced from ECMWF at a resolution of $1/8^\circ \times 1/8^\circ$. This dataset encompasses the u (east–west) and v (north–south) components of the wind vector, along with the sea level pressure.

An unstructured grid, finite volume, regional ocean model FVCOM [45] was used to simulate the hydrodynamic background and hydrological features. It has been widely used for the study of coastal oceanic and estuarine circulation [46–48]. To enhance computational accuracy and reduce computation time, the density of boundary nodes gradually decreases from nearshore to offshore. In the offshore region, the grid density is lower, with a resolution of 0.2 km, while the nearshore part of the open boundary has a higher grid resolution. In the main research area near the river channel, the grid resolution is highest, reaching 50 m. The entire study area grid comprises a total of 25,921 computational nodes (Figure 5). Since the primary focus is on the surface-related hydrodynamic information, the vertical dimension is discretized into five layers. The hydrodynamic model used in this study has been previously validated for its ability to simulate current velocity and direction [49]. In that work, we compared the model outputs with in situ measurements and found a high degree of correspondence, confirming the reliability of the model for our region of interest.

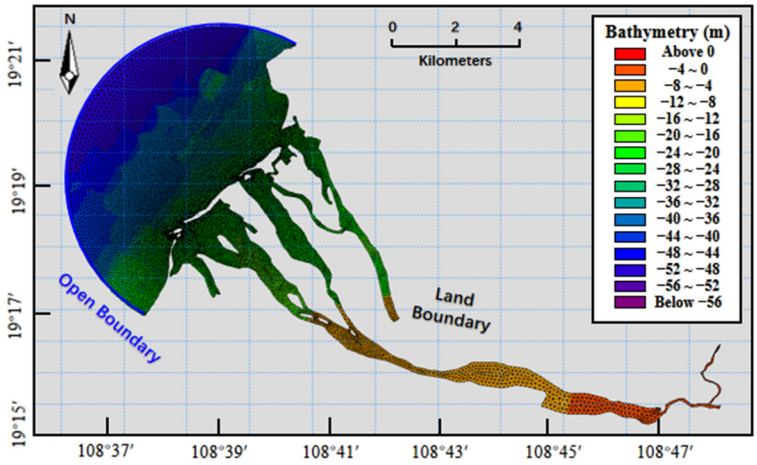

Figure 5. The study and simulation area consisted of a mesh file (mesh triangulation and boundary conditions) and applied in the model: The grid resolution varies from 0.2 km in the offshore region to 50 m in the main research area near the river channel.

4. Results

4.1. Sediment Types

Granulometric analysis results were utilized to construct a distribution map of surficial sediment types (Figure 6d). The study area, encompassing the lower reaches of the Changhua River and the adjacent marine area, exhibits a diverse array of surficial sediment types. These include gravelly sand, silty gravel, sandy silt, silt, sandy gravel, sand, gravelly silt, gravel sand, silty sand, and gravelly muddy sand, among which gravelly sand and gravelly sand are predominant. The overall sediment particle size is relatively coarse, with gravelly sand constituting 30% and gravel sand 17.5% of the sediment types. Silty sand and sand account for 7.5% each, while silt, gravelly muddy sand, and silty gravel each make up 10%. The sediment types in the study area display a patchy distribution pattern, dominated by gravelly sand and gravelly muddy sand. In contrast, the offshore sea area exhibits simpler sediment type distributions with larger distribution areas. The northern sea area (the Beibu Gulf) is primarily characterized by fine-grained sediments such as mud and silty sand; the central area is dominated by coarse-grained sediments like gravelly sand and gravel sand; and the southern sea area is mainly composed of sandy silt.

4.2. Distribution Characteristics of Sediment Grain Size Parameters

The isopleth distribution of the mean grain size of sediments is shown in Figure 6a. The mean grain size of sediment samples in the study area ranges from 0.02Φ to 7.18Φ, with an average value of 3.17Φ. It can be observed that the distribution of the mean grain size of sediments in the study area shows a fine-coarse-fine change from north to south, which is consistent with the trend in the sediment type distribution. This reflects that the hydrodynamic energy in the study area gradually transitions from a low-energy environment in the northern bay to a high-energy environment at the estuary, and then shifts to a low-energy environment in the southernmost part (the Bay direction). Within a 3 km range of the downstream river channel to the estuary, there is a coarse-grained area. Most of the mean grain size of sediments is less than 2Φ, dominated by coarse-grained sediments, and the isopleth lines of 0.4–1.6Φ are distributed in a SE–NW strip, reflecting a general southeast to northwest sediment transport direction. From the estuary extending 3 km outward to the open boundary of the ocean, there is another area of coarse-grained sediments. From the southeast to the northwest, from the downstream river channel to the estuary extending nearly straight to the far sea, the sediments are mainly coarse-grained, reflecting the strong average dynamic force of sediment transport in this area, which is the manifestation of wave convergence and transportation force dominated by waves and wave-generated longshore currents.

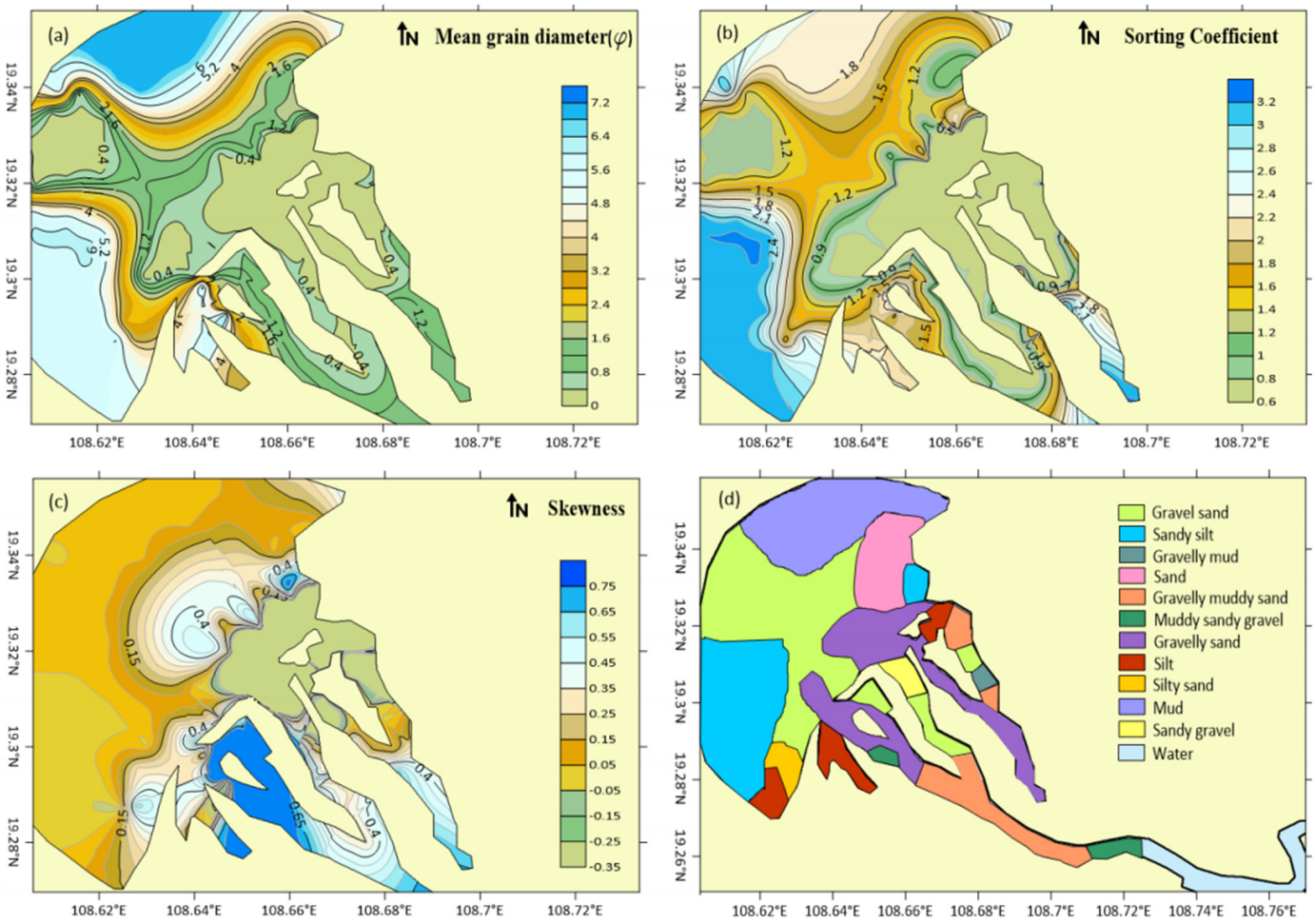

Figure 6. (**a**) Spatial distributions of the mean diameter of the surface sediment. (**b**) Spatial distributions of the sorting coefficient. (**c**) Spatial distributions of the skewness. (**d**) Spatial distributions of the sediment types in the study area.

It can be seen from Figure 6b that the sorting of mud and sand in the study area is between 0.6 and 3.2, which is poor. The sorting coefficient in the main river channel of the lower reaches of the Changhua River is as high as 3.0, and the degree of sorting is very poor. This is because the action of the current is supported by the tide, and the mud and sand are mixed and settle directly without sorting. The sorting coefficient in the southern part of the study area (the Beili Bay direction) is generally greater than 2.4. The region is affected by the current, waves, and tides, with strong hydrodynamic conditions, which can transport particles of different grain sizes together, resulting in a mixture of coarse and fine sediments and poor sorting. The sorting coefficient in the northern part of the study area (the Beibu Gulf) is greater than 1.5, and the degree of sorting is relatively poor, which is better than that in the southern part of the study area. The best sorting area is located in the nearshore area and the far northwest sea area, with a sorting coefficient between 0.6 and 1.2, and the degree of sorting is moderate. Overall, the study area has a high overall sorting coefficient and poor sorting, reflecting the complex material source and hydrodynamic conditions of the area.

It can be seen from Figure 6c that the range of skewness in the study area is from −0.66 to 0.75. The southern part of the study area (Beili Bay) and the B and C estuaries are all negatively skewed, with the median at the finer end and the grain size enriched at the finer end. Most of the remaining areas are positively skewed, with sediments enriched at the coarser end, and the grain size is mainly enriched at the coarser end. The study area's skewness is extremely negatively skewed to extremely positively skewed, and most of the

outer sea of the study area is nearly symmetrical. There is an area with extremely positive skewness at the C estuary.

4.3. Sediment Dynamic Zoning

The dynamic environmental characteristics of surficial sediments in the research area were analyzed using the Flemming triangle diagram method [50], which integrates sediment grain size features and the strength of hydrodynamic forces they represent to delineate sediment dynamic environments and sub-environments. The sediment grain size classification standards in the dynamic zoning map are as follows: sand sediment particles with a diameter of 0.063–2.000 mm, silt from 0.004 to 0.063 mm, and clay less than 0.004 mm. The structural classification lines in the diagram are based on the mass fraction of sand as nodes, at 5%, 25%, 50%, 75%, and 95%, creating six components from S to E, indicating a gradual decrease in sediment particle size from S to E. The fine-grained components (clay and silt) in the sediments are used as classification lines for the triangular structure, at 10%, 25%, 50%, 75%, and 90%, dividing into six hydrodynamic zones from I to VI. The closer to the clay and silt end-members, the weaker the hydrodynamic force; from I to VI, hydrodynamic forces gradually weaken. Thus, the Flemming triangle diagram method divides the triangle into 25 areas, each representing different sediment dynamic environments. Consequently, in the Flemming triangle diagram, the sediment grain size increases from S to E; hydrodynamic environments weaken from I to VI.

Based on grain size parameters, topography, sediment sources, hydrodynamics, and sediment transport, the study area is divided into four sedimentary regions (Figure 7a,b): the Northern Offshore Depositional Zone, Central Offshore Depositional Zone, Southern Offshore Depositional Zone, and Downstream River Channel Depositional Zone.

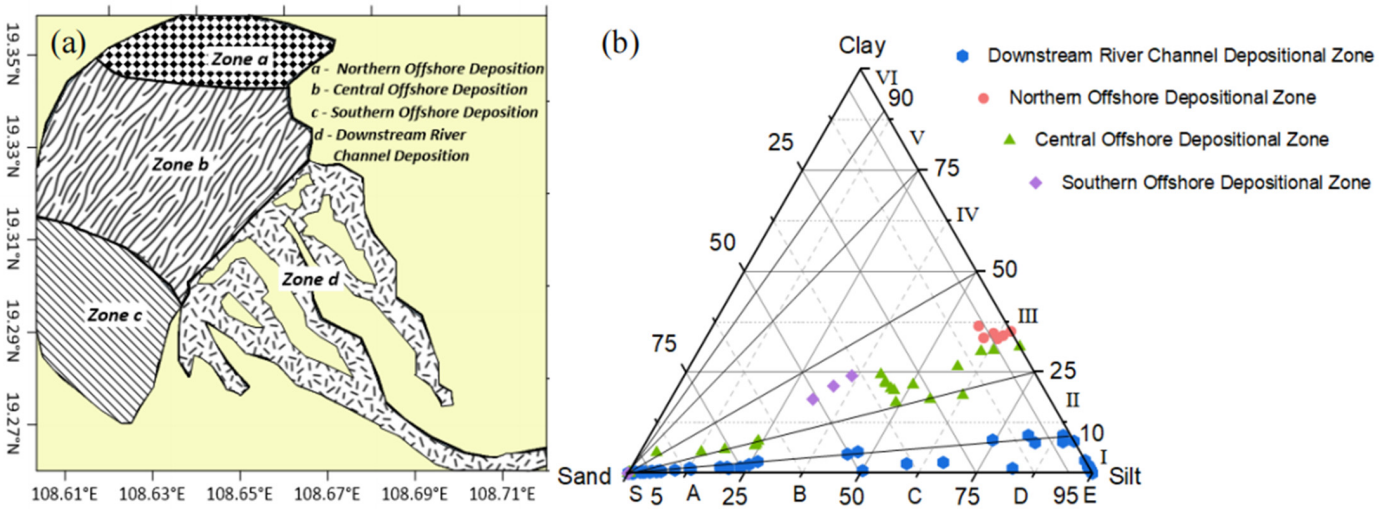

Figure 7. (**a**) Distribution characteristics of sediment classification in the study area. (**b**) Sediment classification according to Flemming triangle diagram: Dividing the study area into four sedimentary regions: Northern Offshore Depositional Zone (red dots), Central Offshore Depositional Zone (green triangles), Southern Offshore Depositional Zone (purple rhombuses), and Downstream River Channel Depositional Zone (blue hexagons).

4.4. Sediment Transport Trend Analysis

In this paper, the GSTA model is used to calculate the grain size transport trends of surficial sediments in the study area based on the spatial distribution of average grain size, sorting coefficient, and skewness (Figure 8). The maximum sampling interval of 2 km is used as the characteristic distance. The vector arrows in the figure represent the net transport direction of sediments, and the length of the vectors indicates the significance of sediment transport, not the rate of sediment transport.

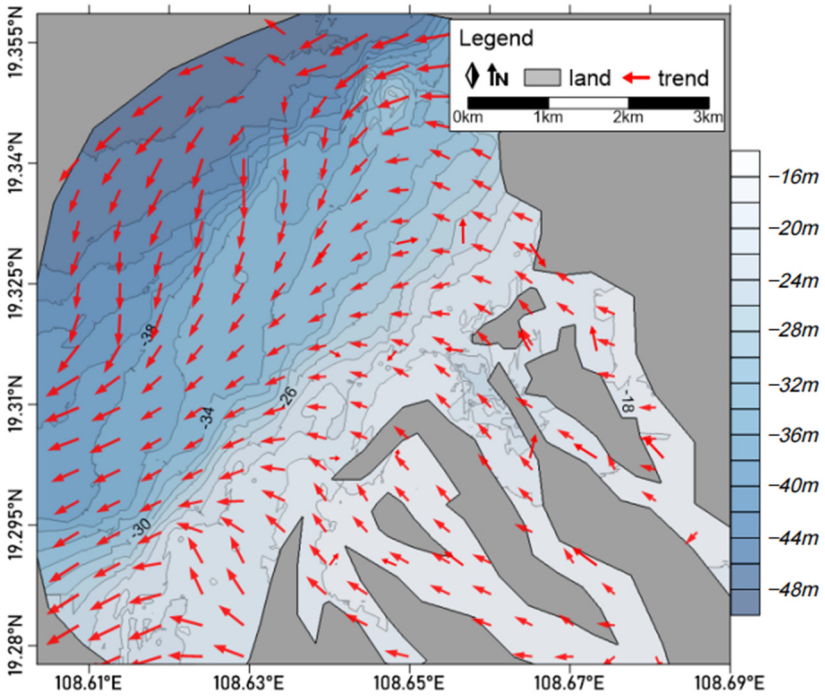

Figure 8. Trends in sediment transport in the Changhua river estuary and downstream areas: The base map is a bathymetric map of the seabed, and the red arrows represent the direction of sediment transport.

The transport trend in surficial sediments from the Changhua River to the nearshore sea area in the study area generally shows a trend from the river to the near sea and then to the far sea. The transport trend at the river outlet is generally strong, mainly moving northwestward after entering the ocean. The transport trend in the near sea is influenced by the combined effects of alongshore currents, residual currents, and rivers. The alongshore current flows in the NE–SW direction, the nearshore residual current flows in the northeast direction, mainly affecting the direction of sediments, and the river mainly flows in the northwest direction. At the southern outlet, affected by both the alongshore current and the river, the sediments gradually change from northwest to southwest; at the central river outlet, affected by the comprehensive influence of seawater, the transport trend changes from northwest to west; at the northern river outlet, affected by the influence of the bay's horn, it moves westward, and after reaching the far sea, the transport direction gradually changes to southwest, consistent with the direction of sediments from other outlets. The overall transport characteristics are northwestward near the sea and southwestward in the far sea. The transport trends of the several distributaries of the Changhua River are the same, all moving towards the ocean. The transport trend in the far sea changes from northwest to south to southwest from north to south. The northwestward transport in the north, together with the circulation of the Beibu Gulf carrying material, will form a deposition center [24,32,33], converging fine-grained sediments, which is consistent with the muddy sediments shown in Figure 2. Under the strong hydrodynamic action of waves, alongshore currents, and runoff, the southwestward transport in the southern far sea will transport coarse particles to Beihai Bay.

5. Discussion

5.1. Implications of Sediment Grain Size Parameters

The fine-coarse-fine change in the mean grain size of sediments from north to south, as observed in the study area, is a direct reflection of the varying hydrodynamic energy. The transition from a low-energy environment in the northern bay to a high-energy environment at the estuary, followed by a shift to a low-energy environment in the southernmost

part, highlights the importance of hydrodynamic forces in shaping sediment distribution. The coarse-grained area within 3 km of the downstream river channel to the estuary, together with the SE–NW strip distribution of isopleth lines, indicates a general southeast to northwest sediment transport direction, which is a significant finding for understanding sediment dynamics in the area.

The poor sorting observed in the study area, with a high overall sorting coefficient, suggests a complex material source and hydrodynamic conditions. The very poor sorting in the main river channel of the lower reaches of the Changhua River, due to the mixing and settling of mud and sand without sorting, is a notable characteristic that impacts sediment transport and deposition processes.

The skewness range in the study area, from extremely negatively skewed to extremely positively skewed, indicates varying sediment enrichment patterns. The negative skewness in the southern part and the B and C estuaries, with enrichment at the finer end, contrasts with the positive skewness in most remaining areas, where sediments are enriched at the coarser end. This variation in skewness provides insights into the sediment transport mechanisms and the influence of different hydrodynamic forces on sediment distribution.

5.2. Sediment Dynamic Zoning and Its Significance

The Flemming triangle diagram method provides a comprehensive framework for analyzing the dynamic environmental characteristics of surficial sediments. The division of the study area into four sedimentary regions based on grain size parameters, topography, sediment sources, hydrodynamics, and sediment transport offers a clear understanding of the sediment dynamic environments and sub-environments. The distribution of sampling points across different zones in the Flemming triangle diagram indicates a dispersed sediment grain size distribution and a predominantly strong overall hydrodynamic force in the study area.

The Northern Offshore Depositional Zone, with its fine sediment particles and low-energy hydrodynamic environment, is likely influenced by the fine-grained material transport of the Beibu Gulf circulation. The Central Offshore Depositional Zone, with its mixture of clay, silt, and sand, suggests moderate hydrodynamic conditions and a broad distribution of sediment grain sizes, influenced by strong tides and seasonal storm tides. The Southern Offshore Depositional Zone, dominated by sandy sediments, indicates a higher-energy hydrodynamic environment and possible influence from distant material inputs. The Downstream River Channel Depositional Zone, with its complex and variable sediment grain size compositions, reflects the diversity of river flow velocity, water depth, and sediment supply sources, showing a strong nature of transition areas.

5.3. Interpretation of Sediment Transport Trends

The sediment transport trends in the study area can be divided into three paths: one from the downstream river channel to the estuary to the southern part of the study area's outer sea; one from the downstream river channel to the estuary to the northern part of the study area's outer sea and then to the southern part of the outer sea; and one from the northern part of the study area's outer sea to the southern part of the outer sea. The first two sediment sources are from the lower reaches of the Changhua River, and the last one is from the Beibu Gulf. This is consistent with previous studies on the sediment transport trends in the lower reaches of the Changhua River [33,35,38,45].

In the estuarine and downstream regions of the Changhua River, climate and water levels exhibit distinct seasonal variations [24,33,38,39,41,42,45], which significantly influence the direction of sediment transport. During the flood season, which corresponds to the summer months, the discharge of the Changhua River increases markedly due to the substantial rise in rainfall, enhancing the river's sediment transport capacity [32,33,42]. During this period, the river carries a substantial load of sediment, leading to increased sediment deposition in the estuary and downstream areas. The faster water flow velocities characteristic of the flood season facilitate the easier transportation and dispersion

of sediment particles near the estuary. Against the backdrop of the prevailing southerly winds in summer, this rapid water flow, in conjunction with the impact of waves and the southwest–northeast coastal current, induces a shift in the sediment transport direction from northwest to southwest. Particularly in the estuarine region, this change is closely related to the intensity of riverine sediment transport and wave action [32,33,45]. Moreover, the high discharge during the flood season may also alter the estuarine topography, creating new erosional channels and depositional areas, which further affect the distribution and transport pathways of the sediment [35,38,45].

In the dry season, which corresponds to spring, the flow of the Changhua River diminishes, leading to a decrease in the river's sediment transport capacity. During this period, the river carries less sediment, and the sediment deposition rate in the estuary and downstream areas is correspondingly reduced. The slower water flow velocities typical of the dry season result in sediment particles being more prone to deposition on the riverbed, leading to more localized and limited sediment transport patterns [32]. Additionally, the low flow during the dry season may enhance the relative significance of wave action in the estuary, exerting a greater influence on the transportation and deposition of sediment. These seasonal variations in water flow and wave action result in different sediment transport characteristics across different seasons. Especially in the estuarine area, the shift in sediment transport direction from northwest to southwest reflects the intensity of riverine sediment transport and wave action during the flood season, as well as the relative enhancement of wave action during the dry season.

To discuss and verify the rationality of the GSTA model calculation results, this paper calculates the surface residual current within 15 synodic days according to the vector synthesis and decomposition method based on the hydrodynamic model results of sea currents, and then uses the drawing tool kit in the Surfer 11 software to draw the residual current distribution map (Figure 9).

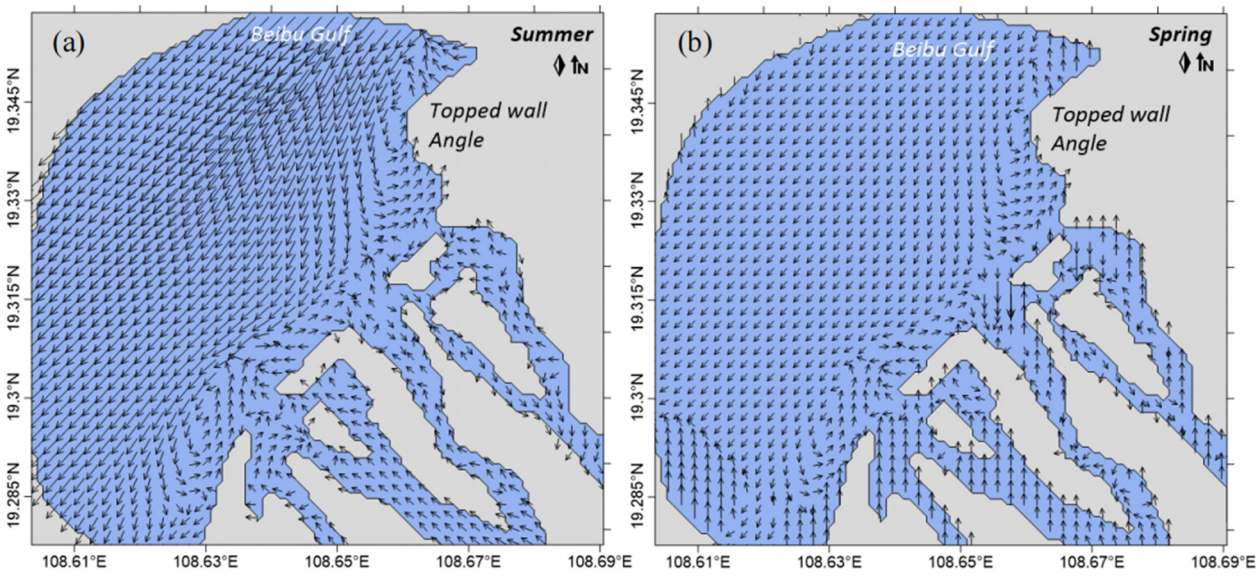

Figure 9. (**a**) Eulerian residual current fields during summer (flood season) (**b**) Eulerian residual current fields during spring (dry season).

There are two vortices in the residual current of the study area, a large counterclockwise vortex in the middle nearshore area, and a small counterclockwise vortex in the southern area. The residual current near the shore flows northeastward, deflects after passing below the topped wall angle, and changes to west–southwestward, moving together with the northwestward residual current from the Beibu Gulf [38]. Most of the residual currents in the far sea are southward and southwestward, and the residual current directions in the river channels all point to the ocean.

Overall, the residual current direction is consistent with the net sediment transport direction of the GSTA model, indicating that the analysis of the sediment transport trend map of the GSTA model is feasible. The main difference is near the shore, where the residual current direction is parallel to the shore and flows northeastward, while the sediment transport direction is parallel to the river channel and flows northwestward. This may be the effect of terrain guidance. The river channel terrain may guide the water flow, causing the water to flow in a specific direction in the river channel. This terrain guidance effect may mask the direct impact of the residual current on sediment transport, causing the sediment transport direction to be inconsistent with the residual current direction. Secondly, the seasonal variation characteristics of the lower reaches of the Changhua River will also lead to inconsistencies between sediment transport and the Euler residual flow field. Although seasonal changes are short-term, they can have a significant impact on long-term sediment transport patterns through long-term cumulative effects. During the flood season, the water flow of the Changhua River increases, carrying a large amount of sediment into the river mouth. These sediments, under the action of strong water flow, may be more easily transported along the river channel direction (or the direction affected by the terrain) and are deposited at the river mouth, thus affecting the morphology and position of the sand spit. During the dry season, the water flow weakens and the amount of sediment carried decreases, but the action of waves and alongshore currents relatively strengthens. These forces may re-transport the already deposited sediment to other locations, causing the sediment transport direction to be inconsistent with the Euler residual current direction.

6. Conclusions

The following conclusions summarize the key findings of our study on sediment transport dynamics in the lower reaches of the Changhua River and its estuary:

Three Main Paths of Sediment Transport: One from the downstream river channel to the estuary to the southern part of the study area's outer sea; one from the downstream river channel to the estuary to the northern part of the study area's outer sea and then to the southern part of the outer sea; and one from the northern part of the study area's outer sea to the southern part of the outer sea. The first two sediment sources are from the lower reaches of the Changhua River, and the last one is from the Beibu Gulf.

Sediment Transport Direction: Sediments in the lower reaches of the Changhua River are primarily transported towards the south and southwest, a trend consistent with Eulerian residual flow patterns, particularly in the offshore areas. Nearshore sediment transport is influenced by the combined effects of alongshore currents, residual flows, and river inputs, leading to complex sediment transport directions.

Mixed Sediment Origins: The sediments in the outer southern part of the study area originate from both the fine-grained materials transported by the circulation of Beili Bay in the north and the coarse-grained materials from the lower reaches of the Changhua River, resulting in a mixed distribution of sediment types in the outer southern part.

Tidal Currents and Sediment Transport: Tidal currents are a significant factor affecting sediment transport, with residual current directions in the outer sea and downstream river channel generally aligning with the net sediment transport directions. However, discrepancies in the nearshore area suggest that the guiding effect of the river mouth sand spit may override the influence of residual currents on sediment transport, causing sediment transport directions to diverge from the residual current flow.

Limitations: In order to assess the sensitivity of the sampling point selection, we conducted additional analyses. By altering the position and quantity of the sampling points, we observed that the results remained robust within a certain range. This suggests that our selection of sampling points is representative to a certain extent, and the study outcomes exhibit a high degree of robustness. However, we also recognize that increasing the number of sampling points, particularly in certain critical areas, may further enhance the representativeness of the results. Future studies could consider augmenting the sampling points in these areas to further validate our findings.

Author Contributions: Conceptualization, Y.W. (Yuxi Wu) and E.Z.; Methodology, Z.X. (Zhiming Xu); Software, Y.W. (Yang Wang) and Q.W.; Validation, X.L., Q.W., D.J. and Z.X. (Zhuang Xing); Formal analysis, Y.W. (Yuxi Wu); Investigation, Y.W. (Yuxi Wu), X.L., Y.W. (Yang Wang), S.Z., Z.X. (Zhiming Xu) and Z.X. (Zhuang Xing); Resources, Y.W. (Yuxi Wu), E.Z., S.Z. and D.J.; Data curation, Y.W. (Yuxi Wu), Y.W. (Yang Wang), S.Z. and Z.X. (Zhiming Xu); Writing—original draft, Y.W. (Yuxi Wu) and E.Z.; Writing—review and editing, Y.W. (Yuxi Wu) and E.Z.; Visualization, Y.W. (Yuxi Wu); Supervision, X.L., E.Z. and Q.W.; Project administration, X.L. All authors have read and agreed to the published version of the manuscript.

Funding: This research was funded by the National Natural Science Foundation of China (Grant Nos. 52371295, 52001286), Guangdong Basic and Applied Basic Research Foundation (Grant No. 2022A1515240002), Hubei Provincial Natural Science Foundation of China (Grant No. 2023AFB576), the Open Fund of Shandong Provincial Key Laboratory of Marine Environment and Geological Engineering (Grant No. MEGE2024006), the China Geological Survey Project (Grant No. DD20220956), and the Fundamental Research Funds for the Central Universities, China University of Geosciences (Wuhan) (Grant Nos. 138-162301212657, 138-162301212679).

Institutional Review Board Statement: Not applicable.

Informed Consent Statement: Not applicable.

Data Availability Statement: Data were obtained from the Haikou Marine Geological Survey Center and are available from the authors with the permission of the Haikou Marine Geological Survey Center.

Conflicts of Interest: The authors declare no conflicts of interest.

References

1. Jiang, F.Y.; Zhao, E.J. Damage mechanism and failure risk analysis of offshore pipelines subjected to impact loads from falling object, considering the soil variability. *Mar. Struct.* **2024**, *93*, 103544. [CrossRef]
2. Sun, Q.L.; Wang, Q.; Shi, F.Y.; Alves, T.; Gao, S.; Xie, X.N.; Wu, S.G.; Li, J.B. Runup of landslide-generated tsunamis controlled by paleogeography and sea-level change. *Commun. Earth Environ.* **2022**, *3*, 244. [CrossRef]
3. Zhao, E.J.; Dong, Y.K.; Tang, Y.Z.; Sun, J.K. Numerical investigation of hydrodynamic characteristics and local scour mechanism around submarine pipelines under joint effect of solitary waves and currents. *Ocean. Eng.* **2021**, *222*, 108553. [CrossRef]
4. Zhao, E.J.; Qu, K.; Mu, L. Numerical study of morphological response of the sandy bed after tsunami-like wave overtopping an impermeable seawall. *Ocean. Eng.* **2019**, *186*, 106076. [CrossRef]
5. Zhao, E.J.; Sun, J.K.; Tang, Y.Z.; Mu, L.; Jiang, H.Y. Numerical investigation of tsunami wave impacts on different coastal bridge decks using immersed boundary method. *Ocean. Eng.* **2020**, *201*, 107132. [CrossRef]
6. Zhao, E.J.; Wu, Y.X.; Jiang, F.Y.; Wang, Y.; Zhang, Z.Y.; Nie, C.H. Numerical investigation on the influence of the complete tsunami-like wave on the tandem pipeline. *Ocean. Eng.* **2024**, *294*, 116697. [CrossRef]
7. Brooks, H.L.; Steel, E.; Moore, M. Grain-Size Analysis of Ancient Deep-Marine Sediments Using Laser Diffraction. *Front. Earth Sci.* **2022**, *10*, 820866. [CrossRef]
8. Dawelbeit, A.; Jaillard, E.; Eisawi, A. Grain size analysis of the latest Quaternary Kordofan Sand of Central Sudan: Depositional environment and mode of transportation. *Aeolian Res.* **2022**, *55*, 100785. [CrossRef]
9. Eltijani, A.; Mohammed, M.A.A.; Abuobida, Y.; Yousif, I.M. Integrating CoDA and PCA for enhanced characterization of fluvial depositional processes: A case study of the Shendi formation, Sudan. *Discov. Geosci.* **2024**, *2*, 10. [CrossRef]
10. Pszonka, J.; Sala, D. Application of the mineral liberation analysis (MLA) for extraction of grain size and shape measurements in siliciclastic sedimentary rocks. *E3S Web Conf.* **2018**, *66*, 02002. [CrossRef]
11. Spychala, Y.T.; Ramaaker, T.A.B.; Eggenhuisen, J.T.; Grundvåg, S.A.; Pohl, F.; Wróblewska, S. Proximal to distal grain-size distribution of basin-floor lobes: A study from the Battfjellet Formation, Central Tertiary Basin, Svalbard. *Depos. Rec.* **2021**, *8*, 436–456. [CrossRef]
12. Syvitski, J.P.; Vorosmarty, C.; Kettner, A.J. Impact of Humans on the Flux of Terrestrial Sediment to the Global Coastal Ocean. *Science* **2005**, *308*, 376–380. [CrossRef] [PubMed]
13. Folk, R.L.; Ward, W.C. A Study in the Significance of Grain-Size Parameters. *J. Sediment. Petrol.* **1957**, *27*, 3–26. [CrossRef]
14. Pszonka, J.; Schulz, B. SEM Automated Mineralogy applied for the quantification of mineral and textural sorting in submarine sediment gravity flows. *Gospod. Surowcami Miner.—Miner. Resour. Manag.* **2022**, *38*, 105–131. [CrossRef]
15. Shideler, G.L.; Ślączka, A.; Unrug, R.; Wendorff, M. Textural and mineralogical sorting relationships in Krosno Formation (Oligocene) turbidites, Polish Carpathian Mountains. *J. Sediment. Petrol.* **1975**, *45*, 44–56.
16. McCave, I.N. Size sorting during transport and deposition of fine sediments: Sortable silt and flow speed. *Dev. Sedimentol.* **2008**, *60*, 121–142. [CrossRef]

17. Paterson, G.A.; Heslop, D. New methods for unmixing sediment grain size data. *Geochem. Geophys. Geosyst.* **2015**, *16*, 4494–4506. [CrossRef]
18. Pszonka, J.; Godlewski, P.; Fheed, A.; Dwornik, M.; Schulz, B.; Wendorff, M. Identification and quantification of intergranular volume using SEM automated mineralogy. *Mar. Pet. Geol.* **2024**, *162*, 106708. [CrossRef]
19. Milliman, J.D.; Syvitski, J.P. Geomorphic/Tectonic Control of Sediment Discharge to the Ocean: The Importance of Small Mountainous Rivers. *J. Geol.* **1992**, *100*, 525–544. [CrossRef]
20. Qi, Y.L.; Yu, Q.; Gao, S.; Li, Z.Q.; Fang, X.; Guo, Y.H. Morphological evolution of river mouth spits: Wave effects and self-organization patterns. *Estuar. Coast. Shelf Sci.* **2021**, *262*, 107567. [CrossRef]
21. Gao, S.; Collins, M.B. Analysis of Grain Size Trends, for Defining Sediment Transport Pathways in Marine Environments. *J. Coast. Res.* **1994**, *10*, 70–78. Available online: https://www.jstor.org/stable/4298194 (accessed on 10 October 2024).
22. Gao, S.; Collins, M.; McLaren, P.; Bowles, D. A critique of the "McLaren Method" for defining sediment transport paths; discussion and reply. *J. Sediment. Res.* **1991**, *61*, 143–147. [CrossRef]
23. Pedreros, R.; Howa, H.L.; Michel, D. Application of grain size trend analysis for the determination of sediment transport pathways in intertidal areas. *Mar. Geol.* **1996**, *135*, 35–49. [CrossRef]
24. Xiao, X.; Shi, Y.H.; Feng, X.L.; Xu, Y.Q. Surface sediment characteristics and dynamics in beibu gulf. *Period. Ocean. Univ. China* **2016**, *46*, 83–89. [CrossRef]
25. Kawakami, G.; Nishina, K.; Poizot, E. Dominant updriftward sediment transport on the updrift-side of a modern deflected delta, Ishikari coast, Hokkaido, Japan. *Mar. Geol.* **2021**, *436*, 106480. [CrossRef]
26. Paladino, I.M.; Mengatto, M.F.; Mahiques, M.M.; Noernberg, M.A.; Nagai, R.H. End-member modeling and sediment trend analysis as tools for sedimentary processes inference in a subtropical estuary. *Estuar. Coast. Shelf Sci.* **2022**, *278*, 108126. [CrossRef]
27. Duman, M.; Eronat, A.H.; Talas, E. Interplay of natural and anthropogenic factors in sediment dynamics and trace element distribution in Güllük Gulf, western Türkiye: A comprehensive geochemical and hydrodynamic analysis. *Cont. Shelf Res.* **2024**, *282*, 105332. [CrossRef]
28. Gao, S.; Collins, M. Net sediment transport patterns inferred from grain-size trends, based upon definition of 'Transport Vector'. *Sediment. Geol.* **1992**, *81*, 47–60. [CrossRef]
29. Gao, S. A FORTRAN program for grain-size trend analysis to define net sediment transport pathways. *Comput. Geosci.* **1996**, *22*, 449–452. [CrossRef]
30. Gao, S. Grain size trend analysis: Principle and applicability. *Acta Sedimentol. Sin.* **2009**, *27*, 826–836.
31. Wright, L.D.; Friedrichs, C.T. Gravity-driven sediment transport on continental shelves: A status report. *Environ. Sci. Geol.* **2006**, *26*, 2092–2107. [CrossRef]
32. Wang, X.M.; Qu, H.B.; Xiong, Y.K.; Lu, L.; Hu, K. Grain-size characteristics and transport trend of bottom sediments at the estuary of Changhua River in Hainan. *Geoscience* **2022**, *36*, 88–95. [CrossRef]
33. Xiao, M.; Wu, J.; Chen, Q.; Jin, M.; Zhang, Y. Dynamic change of land use in changhua downstream watershed based on ca-markov model. *Trans. Chin. Soc. Agric. Eng.* **2012**, *28*, 231–238. [CrossRef]
34. Dai, S.P.; Luo, H.X.; Hu, Y.Y.; Zheng, Q.; Li, H.L.; Li, M.F.; Yu, X. Dynamic Land Use Change of Hainan Island in Recent 20 Years Based on GLC30 Data. *Agric. Eng.* **2021**, *11*, 61–69. [CrossRef]
35. Lu, L. Research of Modern Sediment Transport Model of Changhua River Estuary in Hainan Province. Master's Thesis, China University of Geosciences (Beijing), Beijing, China, 2021. [CrossRef]
36. Hainan Provincial Academy of Environmental Sciences. *Dataset of Hainan Island Ecological System Pattern from 2000 to 2019 (30 m) [Data Set]*; International Research Center for Big Data on Sustainable Development Goals: Beijing, China, 2022. [CrossRef]
37. Xu, D. Sedimentary Records Since Last Deglaciation and the Formation of Modern Sedimentary Pattern in Eastern Beibu Gulf. Ph.D. Thesis, University of Chinese Academy of Sciences, Beijing, China, 2014.
38. Mao, L.M.; Zhang, Y.L.; Bi, H. Modern pollen deposits in coastal mangrove swamps from northern Hainan Island, China. *J. Coast. Res.* **2006**, *22*, 1423–1436. [CrossRef]
39. Wu, J.Q.; Xiao, M.; Yang, J.T.; Xiao, X.B.; Tang, W.H. Study on distribution characteristics of soil erosion in the lower reaches of Changhua River in Hainan. *Technol. Soil Water Conserv.* **2012**, *2012*, 12–15. [CrossRef]
40. Zhang, P.; Ruan, H.M.; Dai, P.D.; Zhao, L.R.; Zhang, J.B. Spatiotemporal river flux and composition of nutrients affecting adjacent coastal water quality in Hainan Island. *J. Hydrol.* **2020**, *591*, 125293. [CrossRef]
41. Zhang, W.Y.; Xiong, P.; Meng, Q.C.; Dudzinska-Nowak, J.; Chen, H.; Zhang, H.; Zhou, F.; Miluch, J.; Harff, J. Morphogenesis of a late Pleistocene delta off the south-western Hainan Island unraveled by numerical modeling. *J. Asian Earth Sci.* **2020**, *195*, 104351. [CrossRef]
42. Zhao, L.; Cai, G.Q.; Zhong, H.X.; Li, B.; Zou, L.Q.; Li, S.; Han, Y.F. Grain-size characteristics and sedimentary environment of surface sediments in the shallow sea in the southeast of Hainan Island. *Mar. Geol. Quat. Geol.* **2021**, *41*, 64–74. [CrossRef]
43. Zhu, L.R.; Liu, Y.H.; Ye, C.Q. Runoff change and influencing factors of Changhua River in arid area of Hainan Island. *Ecol. Sci.* **2020**, *39*, 183–189.
44. Gao, J. Study on Sediment Transport Model in Changhua River Estuary of Hainan Province Based on Remote Sensing Analysis. Master's Thesis, China University of Geosciences (Beijing), Beijing, China, 2014.
45. Chen, C.; Liu, H.; Beardsley, R.C. An unstructured grid, finite-volume, three-dimensional, primitive equations ocean model: Application to coastal ocean and estuaries. *J. Atmos. Ocean. Technol.* **2003**, *20*, 159–186. [CrossRef]

46. Chen, C.; Xue, P.; Ding, P.; Beardsley, R.C.; Xu, Q.; Mao, X.; Gao, G.; Qi, J.; Li, C.; Lin, H.; et al. Physical mechanisms for the offshore detachment of the Changjiang Diluted Water in the East China Sea. *J. Geophys. Res. Ocean.* **2008**, *113*, C02002. [CrossRef]
47. Jiang, L.; Xia, M. Dynamics of the Chesapeake Bay outflow plume: Realistic plume simulation and its seasonal and interannual variability. *J. Geophys. Res. Ocean.* **2016**, *121*, 1424–1445. [CrossRef]
48. Lai, W.; Pan, J.; Devlin, A.T. Impact of tides and winds on estuarine circulation in the Pearl River Estuary. *Cont. Shelf Res.* **2018**, *168*, 68–82. [CrossRef]
49. Wu, Y.; Zhao, E.; Li, X.; Zhang, S. Application of Wave-current coupled Sediment Transport Models with Variable Grain Properties for Coastal Morphodynamics: A Case Study of the Changhua River, Hainan. *EGUsphere* **2024**, preprint. [CrossRef]
50. Flemming, B.W. A revised textural classification of gravel free muddy sediments on the basis of ternary diagrams. *Cont. Shelf Res.* **2000**, *20*, 1125–1137. [CrossRef]